Flexural Performance of Dually Reinforced 3D Concrete Printed Beams

M. van den Heever, F. A. Bester, P.J. Kruger, G.P.A.G. van Zijl

Division for Structural Engineering and Civil Engineering Informatics, Department of Civil Engineering, Stellenbosch University, Stellenbosch, 7602, South Africa.

Marchant van den Heever

PhD Candidate

BEng Civil

RESEARCH FOCUS:

Structural performance of modular 3D concrete printed components under moderate seismic action

THE WORLD'S GATHERING PLACE FOR ADVANCING CONCRETE

aci VIRTUAL CONCRETE CONVENTION

Selecting Suitable Reinforcement Strategies

Cumulative number of papers relating to respective reinforcement strategies

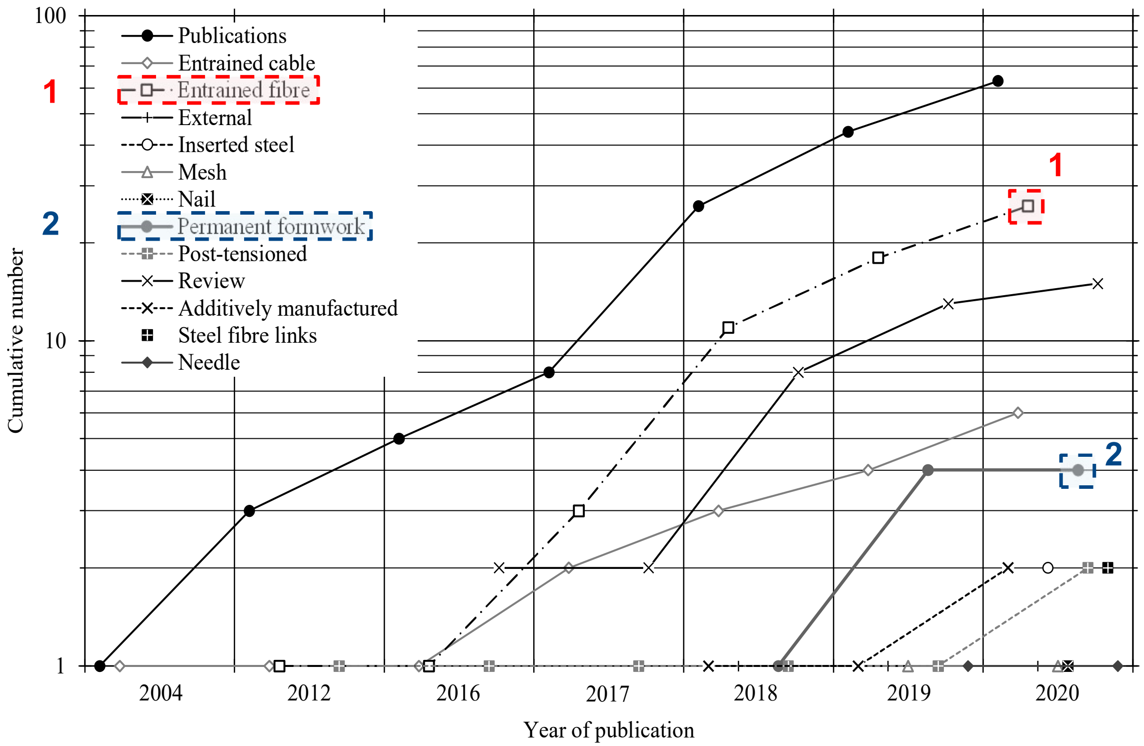

Bester et al., Reinforcing digitally fabricated concrete: A systems approach review, Additive Manufacturing, 2020

Selected Strategies

1. **Entrained fibres**
   - **Most publicised strategy**
   - **High level of compatibility**
   - **Ease of application**
2. **Permanent formwork**
   - **3rd most publicised strategy**
   - **Most often implemented in practice**
   - **Readily available**

Dual Reinforcement Strategy

6mm entrained HM-PP microfibres

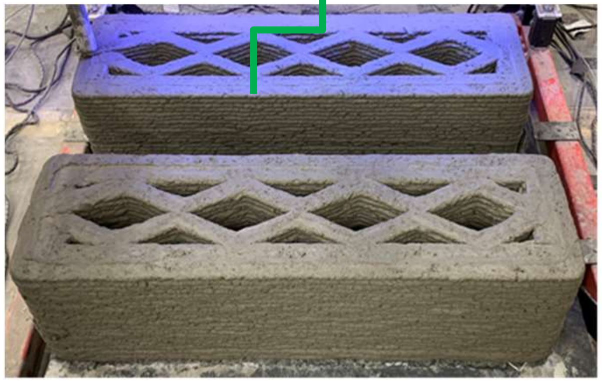

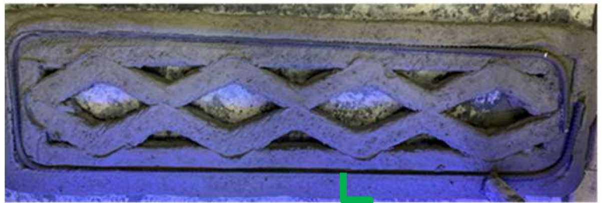

Y10 in-laid conventional reinforcement

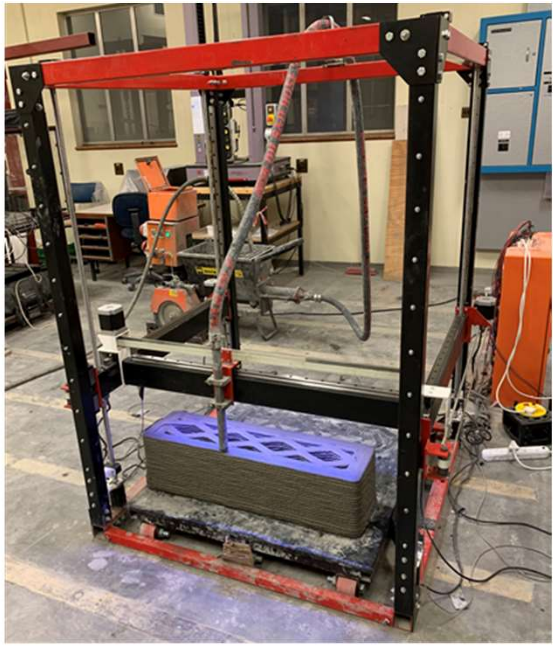

FRPC mixture constituent proportions

Constituent	kg
PPC Suretech CEM II/A-L 52.5 N	562
Durapozz Fly Ash (Class F)	162
Micro Silica Fume	81.4
Fine Aggregate (Malmesbury)	1144
Water	256
Superplasticizer	0.6% by binder mass
VMA	0.3% by binder mass
6 mm HM-PP Microfibres	1% by mixture volume

HM-PP microfibre properties

Description	Value
Young's Modulus (E_f)	30 GPa
Yield Stress (f_t)	1200 MPa
Diameter (d)	15 µm
Length (L)	6 mm

Loading Configurations

Configuration 1

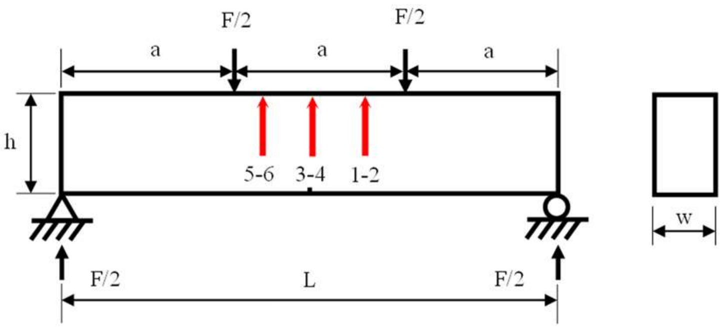

Configuration 3

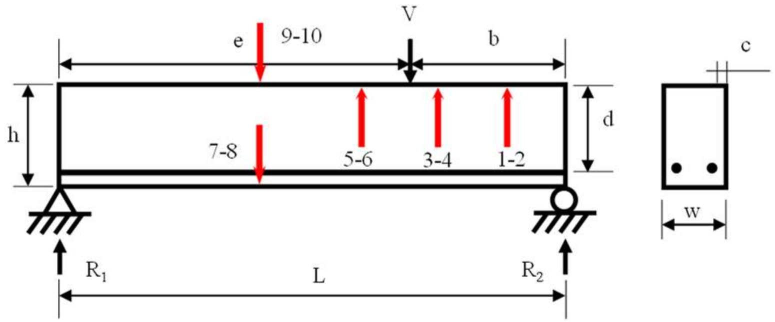

Summary of dimensions used

Dim.	Value	Units	Dim.	Value	Units
a	280	mm	**e**	502	mm
b	338	mm	**h**	260	mm
c	25	mm	**w**	260	mm
d	230	mm	**L**	840	mm

Configuration 2

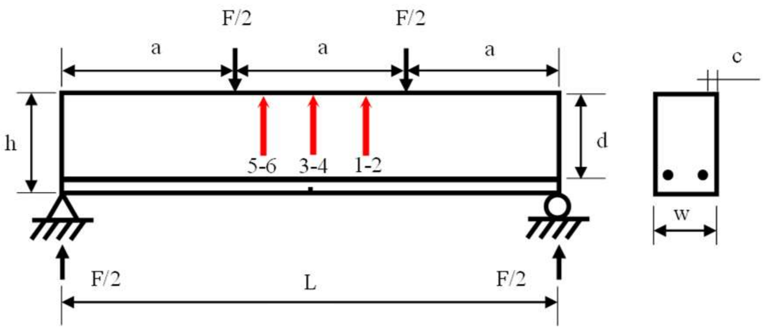

Member & LVDT Frame

Experimental Results

Configuration 1

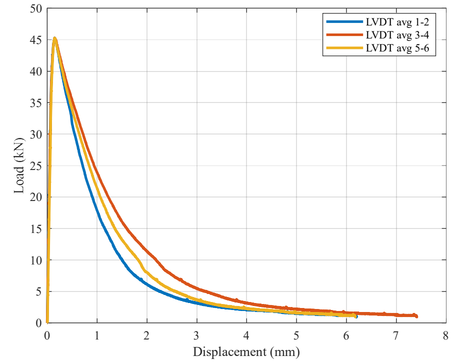

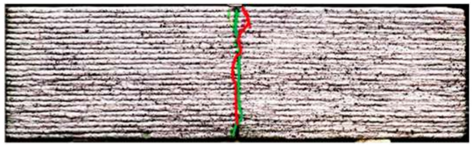

- Ultimate bending capacity = **45.3 kN.**
- Maximum mean mid-span deflection = **7.4 mm.**
- **Strain-softening** post-peak response displayed.
- **Symmetric single vertical bending crack.**

Configuration 2

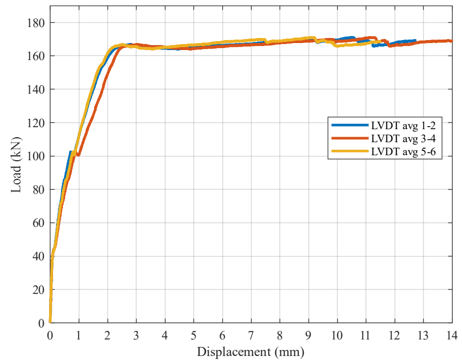

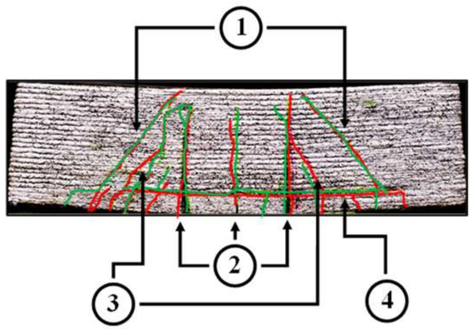

- **3.6 x** Amplified load-carrying capacity.
- **No** noticeable **bond-slip** or **pull out** between rebar & printed matrix.

1. **103 kN**: **Diagonal shear crack**, thus shear dominant failure.
2. **164 kN**: Limited deformability of printed matrix → Strain localisation → **rebar yields.**
3. **Multiple smaller flexural cracks**: Increased deformation + strain redistribution.
4. **Interlayer delamination**: Excessive deformation & curvature.

Configuration 3

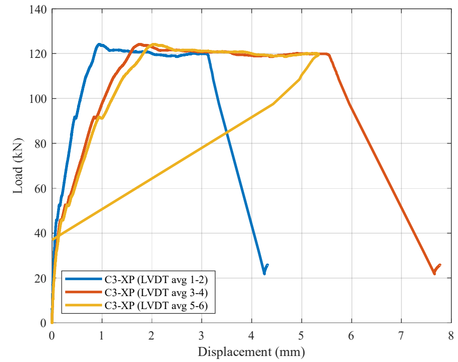

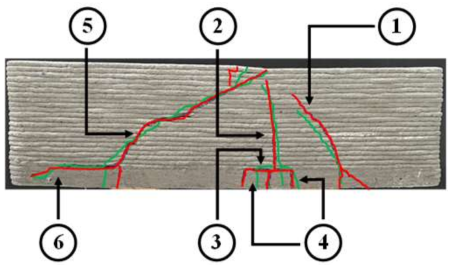

1. **93 kN: Diagonal shear crack**, thus shear dominant failure.
2. **124 kN: Vertical bending crack** → rebar yields → plateau.
3. **Interlayer delamination**: Excessive deformation & curvature.
4. **Smaller flexural cracks**: Increased deformation + strain redistribution.
5. **Brittle ult. failure: shear-flexure crack**: lack of shear links.
6. **Horizontal crack**: debonding due to cracking, large curvature & reduced contact area on location of rebar placement.

Numerical Simulation Frameworks

Expected Failure Mechanisms in 3DCP Elements

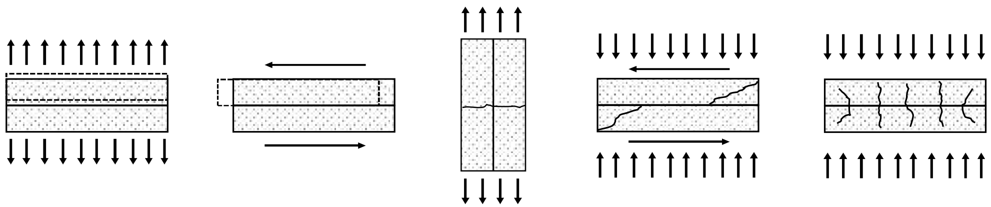

Interfacial cracking | Interfacial shear-slip | Matrix tensile cracking | Matrix cracking: compression-shear | Crushing

Continuum Model

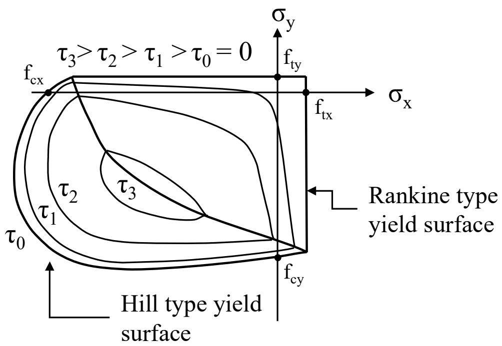

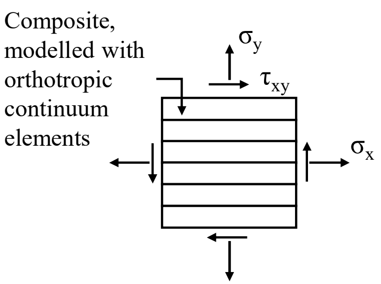

Discrete Interface Model

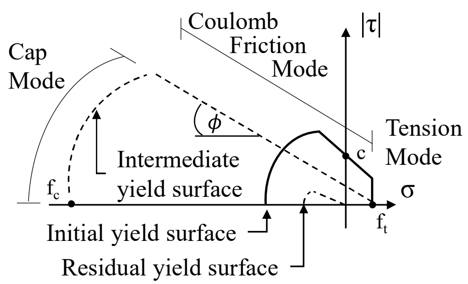

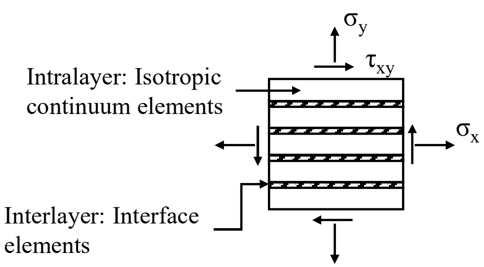

2D Plane Stress Simplification

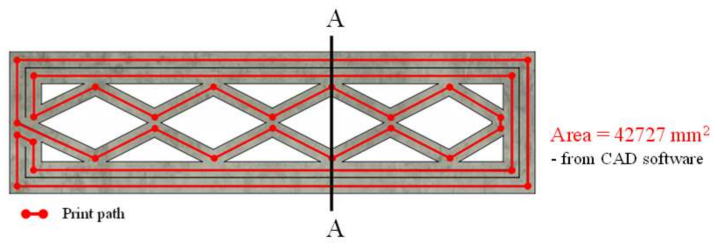

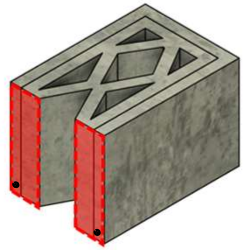

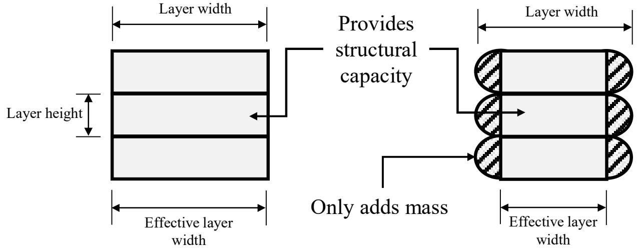

Calculating the Effective Plane Stress Thickness

$$\boldsymbol{t} = \frac{A_{\sec A-A}}{h} = \frac{42727}{260} = \mathbf{164\ mm}$$

$$\Delta_{CF} = \frac{L_{w,eff}}{L_w} = \frac{26}{30} = \mathbf{0.86}$$

$$\boldsymbol{t_{eff}} = \Delta_{CF} \cdot t = \mathbf{141\ mm}$$

Numerical Simulation Parameters: Continuum Model

Model Description:

To exploit the **anisotropic Rankine-Hill continuum model** available in the **DIANA FEA** package, two elastic parameters (E, ν), seven strength parameters (f_{tx}, f_{ty}, f_{cx}, f_{cy}, α, β, and γ), and five inelastic parameters (G_{fx}, G_{fy}, $G_{fc,x}$, $G_{fc,y}$, and κ_p) are required.

Summary of Parameters

Isotropic Elastic Parameters					
E	21.9	GPa	ν	0.2	-
Orthotropic Strength Parameters					
	x-direction			**y-direction**	
f_{tx}	2.45	N/mm^2	f_{ty}	1.25	N/mm^2
f_{cx}	45.1	N/mm^2	f_{cy}	38.2	N/mm^2
Unitless Strength Parameters					
α	0.35	β	-1	γ	0.525
Orthotropic Inelastic Parameters					
Crack bandwidth		User Specified			
G_{fx}	0.956	N/mm	G_{fy}	0.063	N/mm
$G_{fc,x}$	27.07	N/mm	$G_{fc,y}$	26.17	N/mm
κ_p	0.002	mm/mm			

van den Heever et al., Mechanical Characterisation for Numerical Simulation of Extrusion-based 3D Concrete Printing, Journal of Building Engineering, in Review, 2021a.

Shear stress contribution to tensile failure

$$\alpha = \frac{f_{tx} \cdot f_{ty}}{\tau_u^2}$$

τ_u is the interface shear-slip (Mode 2) capacity equal to 2.96 MPa

Shear stress contribution to compressive failure

$$\gamma = \frac{f_{cx} \cdot f_{cy}}{\tau_u^2}$$

τ_u is the material pure shear (Mode 2) strength equal to $1.5f_{c,y}$ MPa

Coupling of normal stress values for compressive failure

$$\beta = -1$$

Default assumed in the absence of experimental data

Numerical Simulation Parameters: Discrete Interface-based Model

Model Description:

The **combined-cracking-shearing-crushing (CCSC) interface model** available in **DIANA FEA** is implemented to define the **IRs** in the 3DCP composite. The **intralayer filaments** are prescribed an **isotropic hypo-elastic total strain-based rotating crack (TSC)** constitutive relation, also available in the **DIANA FEA** package.

Summary of Parameters

Interface Parameters (CCSC)			**Continuum Parameters (TSC)**		
Parameter	**Value**	**Units**	**Parameter**	**Value**	**Units**
$f_{t,j}$	1.25	N/mm^2	E	21900	N/mm^2
$G^I_{f,j}$	0.063	N/mm	v	0.2	-
c_c	2.96	N/mm^2	ρ	2.15E-06	T/mm^3
Friction angle (φ)	36.87	degree	Crack orientation	Rotating	
Dilatancy angle (ψ)	0	degree	Tensile curve	Exponential	
Res. friction angle (φ_r)	36.87	degree	f_t	2.45	N/mm^2
Conf. normal stress	-1	N/mm^2	G^I_f	0.956	N/mm
Exp. Deg. Coeff.	1	-	Crack bandwidth	User specified	
G^{II}_{fc}	0.296	N/mm	Poisson ratio reduction	Damage based	
G_{cc}	26.17	N/mm	f_c	45.1	N/mm^2
k_{nc}	1.00E+06	N/mm^3	G_{cc}	27.07	N/mm
k_{sc}	4.17E+05	N/mm^3			
$c_{ss,j}$	3.5	-	Reduction due to lateral cracking		No
$f_{c,j}$	38.2	N/mm^2	Confinement increase		No
κ_p	0.01	N/mm^2			

van den Heever et al., Numerical Modelling Strategies for Reinforced 3D Concrete Printed Elements, Additive Manufacturing, in Review, 2021b.

Numerical Simulation Results: Continuum Model

Configuration 1

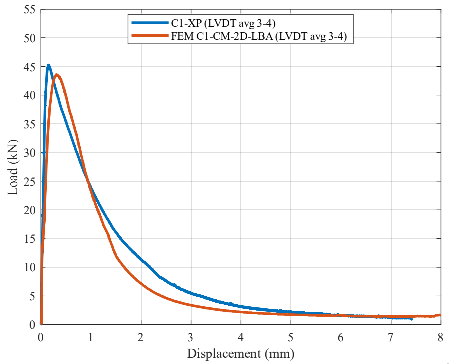

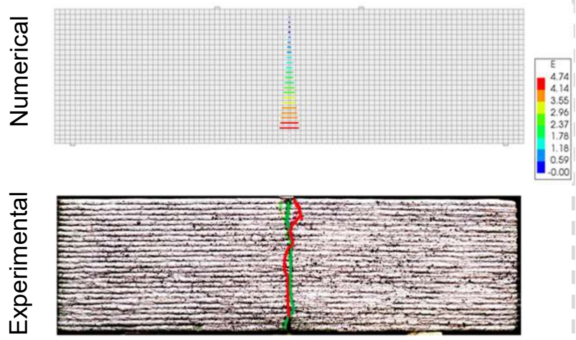

- Ultimate bending capacity = **43.6 kN (-3.8% under estimation LBA parameters),** good agreement in post peak regime.
- **Single vertical bending crack** as in experimental results.

Configuration 2

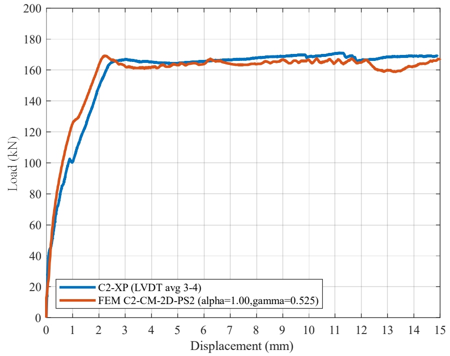

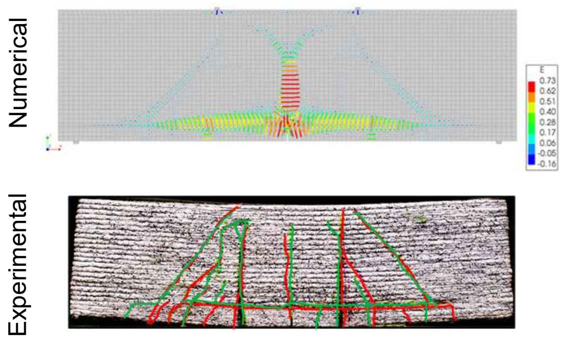

- Presenting selected result of parameter study **(α = 1, γ = 0.525).**
- **Initial shear capacity = 125 kN, diagonal shear failure (+21% over estimation of shear capacity).**
- **Flexural capacity = 169 kN, central bending failure (+3% over estimation) –** crack pattern has reasonable agreement, besides the localisation of the central bending crack.

Configuration 3

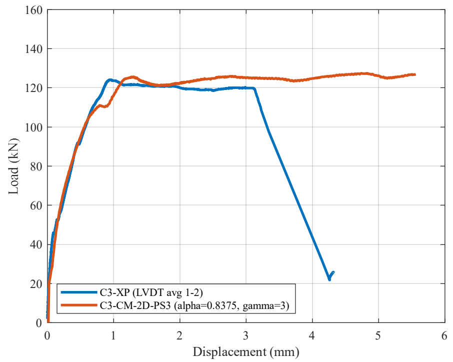

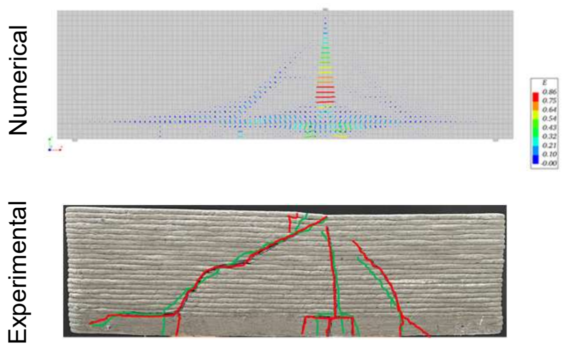

- Presenting selected result of parameter study **(α = 0.84, γ = 3).**
- **Initial shear capacity = 111 kN, diagonal shear failure towards bottom right.**
- **Flexural capacity = 125.2 kN, central bending failure (+1% over estimation) –** crack pattern has good agreement, capturing all major failure modes.
- Although, ultimate failure is misrepresented.

Numerical Simulation Results: Discrete Interface-based Model

Configuration 1

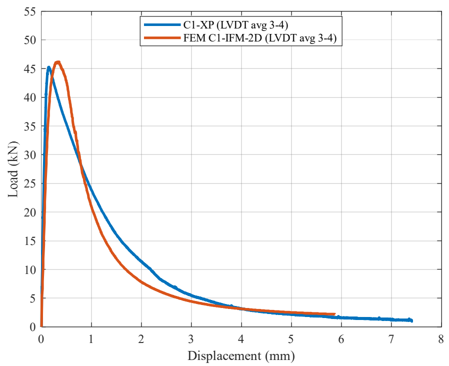

Numerical

Experimental

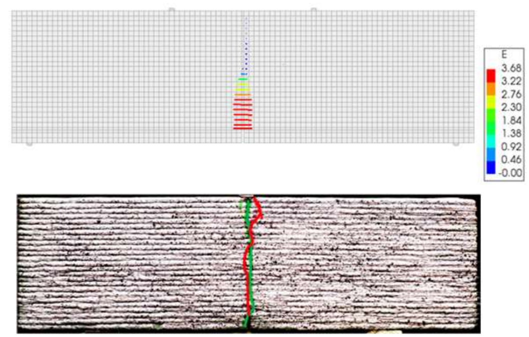

- Ultimate bending capacity = **46.2 kN (+2% over estimation with STD parameters),** good agreement in post peak regime.
- **Single vertical bending crack** as in experimental results.

Configuration 2

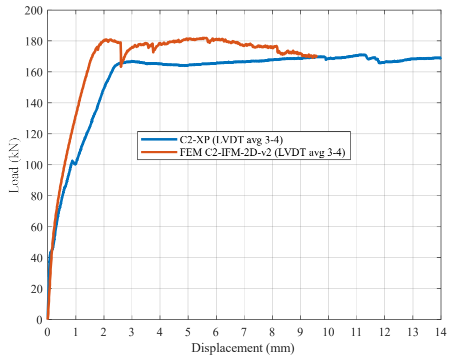

Numerical

Experimental

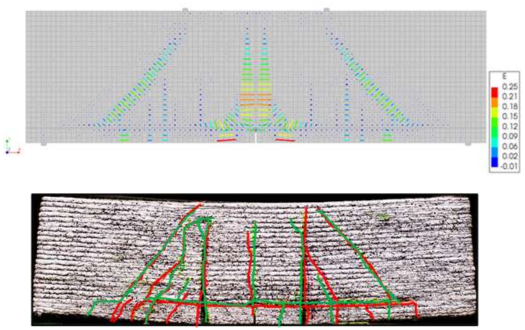

- Ultimate capacity = **181 kN (+9% over estimation STD parameters),** reasonable agreement in post peak regime.
- **Crack pattern is particularly well represented, capturing all major failure modes**

Configuration 3

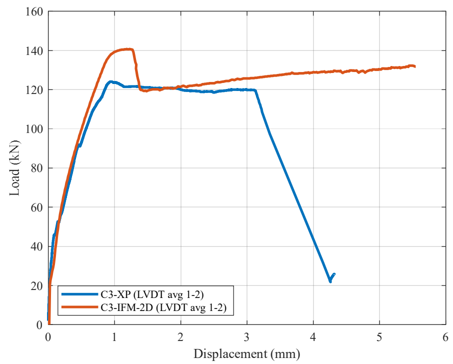

Numerical

Experimental

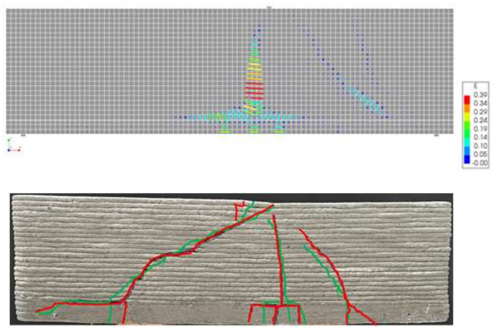

- **Ultimate capacity = 141 kN, central bending failure (+14% over estimation) –** incorrect crack pattern , only captures shear and flexural failure and disregards shear-flexural failure.
- This explains the post-peak hardening shown.
- Additional calibration of shear parameters is required.

Conclusions

- **Both entrained fibre & in-laid reinforcement methods are compatible with 3DCP**
- **In-laid reinforcement** provides **3.6 x amplified load-carrying capacity** (ρ_s **= 0.43%**) attributed to strain-hardening, displays **sufficient bond** and **anchorage**, permitting **strain redistribution** and **providing ductility**.
- **Strain-softening** in observed for the **singularly reinforced** beam while **strain-hardening** for **dually reinforced** member
- **Pure bending** of **singularly reinforced** members is accurately simulated by both numerical simulation strategies (peak load capacity **< 4%** & **excellent agreement** shown in **cracking patterns** and **softening regimes**).
- **Pure bending** of **dually reinforced** members is accurately simulated by both numerical simulation strategies (peak load capacity **< 9%** & **respectable agreement** shown in **cracking patterns** and **post-peak regimes**).
- **Reasonable agreement** is observed under **eTPB** (exhibiting a maximal load capacity **<= 14%**).
- From the numerical results it is evident that the **shear stress is over estimated** and **additional experimental calibration** is required.
- The **similarities** in both the **force-displacement response** and **crack patterns** attained across all simulations indicate that the respective **FE simulation strategies apply to 3DCP**

Flexural Performance of Dually Reinforced 3D Concrete Printed Beams

M. van den Heever, F. A. Bester, P.J. Kruger, G.P.A.G. van Zijl

Division for Structural Engineering and Civil Engineering Informatics, Department of Civil Engineering, Stellenbosch University, Stellenbosch, 7602, South Africa

Thank You!

mvdheever@sun.ac.za

THE WORLD'S GATHERING PLACE FOR ADVANCING CONCRETE

aci VIRTUAL CONCRETE CONVENTION